

# Optimization of Semi-Active Control of Seismically Excited Buildings Using Genetic Algorithms

S. Pourzeynali<sup>1,\*</sup> and T. Mousanejad<sup>1</sup>

**Abstract.** *In this paper, the performance of semi-active viscous dampers in reducing the response of tall buildings to earthquake acceleration is optimized using genetic algorithms. Torsional effects due to irregularities exist in the building and due to unsymmetrical placement of the dampers are taken into account through 3-D modeling of the building. For the numerical example, a twelve-story building is chosen. The building is modeled as a 3-D frame. The equations of motion of the building with semi-active viscous dampers, subjected to earthquake acceleration, is written, resolved in state space and the results are compared with those of the uncontrolled building. Moreover, in order to minimize building responses such as top story displacement and base shear, the required number and location of dampers are optimized using genetic algorithms.*

**Keywords:** *Optimization; Genetic algorithms; Fluid viscous damper; Semi-active control.*

## INTRODUCTION

A large amount of energy is imported into a structure during earthquake ground motion. Conventional design philosophy prevents collapse by allowing structural members to absorb and dissipate the transmitted earthquake energy using inelastic cyclic deformations in specially detailed regions. Consequently, depending on the extent of the design, damage to parts or all of the structure may occur, possibly such that the structure is no longer repairable.

During the last decades, many control systems have been developed to enhance safety and reduce damage to structures during earthquakes [1-3]. These alternative approaches aim to control the structural seismic response and energy dissipation demand on the structural members by modifying the dynamic properties of the system.

Many research studies have shown that the control systems are highly effective in reducing the response of structures subjected to earthquake excitations. Three main categories of these control systems are passive, semi-active and active devices. Various

types of control system have been developed and experimentally verified. A number of them have been implemented in full scale civil structures [4].

Among these control systems, semi-active control has received considerable attention from the civil engineering community in recent years [5-8], because it has the adaptability of active control devices without the need of large input energy as well as the reliability of passive devices. Preliminary analytical and experimental studies indicate that appropriately implemented semi-active systems perform significantly better than passive devices [9-12] and have the potential to achieve or even surpass the performance of fully active systems [13].

By using a small external power, a semi-active device dynamically changes parameters, such as either damping or stiffness coefficients, and produces a large control force [14]. Control forces are developed based on feedback from sensors that measure the excitation and/or the response of the structure [15].

To date, many variable semi-active structural control systems have been proposed and some have been implemented in real structures. Examples include variable stiffness devices, Electrorheological (ER) dampers, Magnetorheological (MR) dampers, semi-active fluid viscous dampers, semi-active tuned mass dampers, and semi-active tuned liquid dampers. Among these devices, the use of semi-active fluid viscous dampers is

1. Department of Civil Engineering, Faculty of Engineering, University of Guilan, Rasht, P.O. Box 41635-3756, Iran.

\*. Corresponding author. E-mail: pourzeynali@guilan.ac.ir

Received 15 May 2009; received in revised form 30 August 2009; accepted 30 November 2009

considered to be a reliable strategy for enhancing the seismic performance of building structures.

In this paper, the performance of semi-active fluid viscous dampers in reducing the response of buildings to earthquake excitations is optimized using genetic algorithms. For this purpose, the building is modeled as a 3-D frame and, then, by employing an analytical procedure, the equations of motion of the building with added semi-active fluid viscous dampers are written. Torsional effects due to irregularities exist in the building and due to the unsymmetrical placement of the dampers are taken into account through 3-D modeling of the building. The viscous dampers are modeled by a linear spring-dashpot connected in parallel. Then, employing a state-space model and a Linear Quadratic Regulator (LQR) control algorithm, the responses of a semi-actively controlled building are obtained.

Furthermore, it is quite important to know that damper configuration can have a significant effect on the structural response to earthquake excitations. For many building structures, the optimal configuration of dampers may provide considerable performance improvement or cost saving. So, in this paper, Genetic Algorithms (GAs) are used to find the optimal number and distribution of semi-active fluid viscous dampers in the model of the building to minimize building responses such as top story displacement, acceleration and base story shear force. For numerical study, a 12-story building located in the city of Rasht, in Iran, is chosen.

## ASSUMPTIONS

The following simplified assumptions are made in this study:

- The building is assumed to have linear behavior during earthquake excitation and therefore, no material nonlinearity is considered in the analyses;
- All floors of the building are assumed to be rigid in plane and flexible for out of plane-bending;
- The building is modeled as a 3-D frame structure, having two lateral and one rotational degree(s) of freedom in the mass center of each floor;
- The structure is analyzed under two horizontal components of the earthquake ground motion, simultaneously;
- The behavior of the fluid viscous damper is assumed to be linear.

## SEMI-ACTIVE FLUID VISCOUS DAMPER

The force-velocity relationship for a fluid viscous damper is represented as:

$$F = CV^n, \quad (1)$$

where  $F$  is the damping output force;  $V$  is the relative velocity of the piston head;  $C$  is damping constant coefficient; and  $n$  is a constant exponent, which depends upon the shape of the piston head. The value of  $n$  is usually between 0.3 and 1.0 [16].

Passive fluid viscous dampers were installed in the newly-constructed San Bernardino County Medical Center in California as components in the rubber bearing, seismic isolation system [17].

A semi-active fluid damper can be achieved by adding an external bypass loop, which contains a controllable valve, to a passive fluid damper. The concept of applying this kind of variable-damping device to control the motion of bridges experiencing seismic motion was first introduced by Feng and Shinozuka [18] and Kawashima et al. [19]. The behavior of the semi-active fluid damper is essentially similar to a passive fluid damper, except that the semi-active fluid damper has an external valve that connects two sides of the cylinder and modulates the output force. The output force is described by [20]:

$$F = C(t)V^n, \quad (2)$$

where  $C(t)$  is the damping time-varying coefficient. The maximum capacity (force  $F$ ) of the dampers used in this study is limited to 1000 kN.

In this kind of damper, an adjustable damping property makes it capable of generating a wide range of damping forces. Since this is a small power or source just used for closing or opening the external valve, it can produce a very large damping force without the need of large input energy and can, therefore, operate on batteries. Shaking table tests indicate that this type of semi-active device can significantly increase the energy dissipation capability of structures with low damping [21].

The first full implementation of a semi-active fluid viscous damper was on the Walnut Creek Bridge on Interstate Highway I-35, in Oklahoma, in order to reduce vehicle-induced vibrations [22]. A similar device has also been studied by Constantinou and Symans [23]. Also, Kurata et al. installed full-scale semi-active fluid viscous dampers in a five-story steel structure in the Kajima, Shizuoka building in Shizuoka, Japan. More recently, these dampers have been installed in some new buildings in the Tokyo Siodome area [24]. Response analysis has shown that this system can significantly reduce both story shear forces and drifts [14].

## SEMI-ACTIVE CONTROL OF BUILDINGS WITH FLUID VISCOUS DAMPERS

In this paper, the response analysis of a three dimensional (3-D) model of multi-story buildings with

added semi-active fluid viscous dampers is studied. Therefore, torsional effects due to irregularities exist in the building and due to unsymmetrical placement of the added dampers can be taken into account.

For buildings subjected to multi-component earthquake excitations, the equation of motion (without any damper) is represented as [25]:

$$\mathbf{M}\ddot{\mathbf{U}} + \mathbf{C}\dot{\mathbf{U}} + \mathbf{K}\mathbf{U} = -\mathbf{M}\mathbf{l}\ddot{\mathbf{U}}_g(t), \quad (3a)$$

$$\ddot{\mathbf{U}}_g(t) = \begin{Bmatrix} \ddot{u}_{gx}(t) \\ \ddot{u}_{gy}(t) \\ 0 \end{Bmatrix}, \quad (3b)$$

where  $\mathbf{M}$ ,  $\mathbf{K}$ , and  $\mathbf{C}$  are structural mass, stiffness, and damping matrices, respectively;  $\mathbf{U}$ ,  $\dot{\mathbf{U}}$ , and  $\ddot{\mathbf{U}}$  are displacement, velocity and acceleration vectors;  $\mathbf{l}$  is the  $N \times N_g$  influence matrix;  $\ddot{u}_{gx}$  and  $\ddot{u}_{gy}$  are earthquake ground accelerations in  $x$  and  $y$  directions, respectively; and  $N$  and  $N_g$  are the number of DOFs of the superstructure and support-excitation components, respectively.

Semi-active fluid viscous dampers can be designed for both new and existing buildings. They are installed between floors in connection with diagonal members or tied into chevron braces. In the present study, dampers are placed in diagonal braces.

The dynamic behavior of these kinds of damper can be expressed by a variable damping coefficient,  $C(t)$ , and an elastic spring in parallel. Their behavior is represented by considering two degrees of freedom per node in the global coordinates (Figure 1a) [26], and by assuming the floors are to be rigid. When the  $j$ th semi-active fluid viscous damper is connected with a

diagonal brace between  $(i-1)$ th and  $i$ th floors on a  $x-z$  plane, its lateral displacement on the  $i$ th floor and in the  $x$  direction can be represented as (Figure 1b):

$$(u_{jx})_i = (e_{yj})_i(u_\theta)_i + (u_x)_i, \quad (4)$$

where  $(e_{yj})_i$  is the offset of the  $j$ th damper from the mass-center of the  $i$ th floor in a  $x$  direction;  $(u_x)_i$  and  $(u_\theta)_i$  are the lateral displacement in  $x$  direction and rotational displacement about the  $z$  axis, both for the mass-center of the  $i$ th floor, respectively. For a damper placed on the  $y-z$  plane, Equation 4 is to be changed to:

$$(u_{jy})_i = (e_{xj})_i(u_\theta)_i + (u_y)_i, \quad (5)$$

where  $(e_{xj})_i$  is the offset of the  $j$ th damper from the mass-center of the  $i$ th floor in the  $y$  direction;  $(u_y)_i$  and  $(u_\theta)_i$  are the lateral displacement in the  $y$  direction and rotational displacement about the  $z$  axis, both for the mass-center of the  $i$ th floor, respectively.

Based on Equations 4 and 5 and condensing vertical degrees of freedom, the time-varying damping matrix,  $\mathbf{C}_{Dj}(t)$ , of the  $j$ th damper placed on the  $x-z$  plane can be written as:

$$\mathbf{C}_{Dj}(t) = c_{dj}(t) \times \begin{bmatrix} \cos^2 \alpha & -\cos^2 \alpha & (e_{yj})_{i-1} \cos^2 \alpha & -(e_{yj})_i \cos^2 \alpha \\ -\cos^2 \alpha & \cos^2 \alpha & -(e_{yj})_{i-1} \cos^2 \alpha & (e_{yj})_i \cos^2 \alpha \\ (e_{yj})_{i-1} \cos^2 \alpha & -(e_{yj})_i \cos^2 \alpha & (e_{yj})_{i-1}^2 \cos^2 \alpha & -(e_{yj})_i(e_{yj})_{i-1} \cos^2 \alpha \\ -(e_{yj})_{i-1} \cos^2 \alpha & (e_{yj})_i \cos^2 \alpha & -(e_{yj})_{i-1}(e_{yj})_i \cos^2 \alpha & (e_{yj})_i^2 \cos^2 \alpha \end{bmatrix}, \quad (6)$$

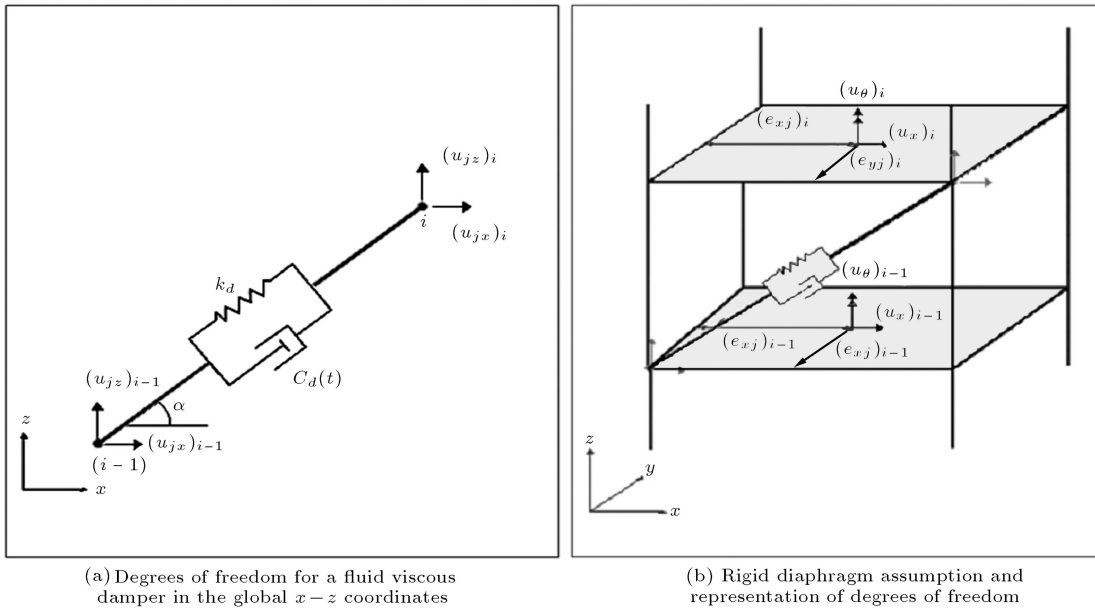


**Figure 1.** Degrees of freedom for fluid viscous damper and rigid diaphragm assumption.

where  $c_{dj}(t)$  is the variable damping coefficient of the  $j$ th damper, and  $\alpha$  is the angle of the damper with a horizontal axis. It is noted that the  $\mathbf{C}_{Dj}(t)$  matrix is written on the basis of the super-structure, mass-center degrees of freedom (DOFs);  $(u_x)_{i-1}$ ,  $(u_\theta)_{i-1}$ ,  $(u_x)_i$ ,  $(u_\theta)_i$  (refer to Figure 1b).

Then, by assembling the condensed matrix of each damper into the total structural damping matrix of the building, the equation of motion of the building with added fluid viscous dampers can be obtained. By using this method, when damper  $j$  is added to a diagonal brace of the building, between  $(i-1)$ th and  $i$ th floors on the  $x-z$  plane, time-varying damping forces produced in lateral and rotational degrees of freedom of  $(i-1)$ th and  $i$ th floors, respectively, can be evaluated as:

$$\begin{aligned} (f_x)_{i-1} &= c_{aj}(t) \cos^2 \alpha [(\dot{u}_x)_{i-1} - (\dot{u}_x)_i \\ &\quad + (e_{yj})_{i-1}(\dot{u}_\theta)_{i-1} - (e_{yj})_i(\dot{u}_\theta)_i], \end{aligned} \quad (7a)$$

$$\begin{aligned} (f_x)_i &= c_{dj}(t) \cos^2 \alpha [-\dot{u}_x]_{i-1} + (\dot{u}_x)_i \\ &\quad - (e_{yj})_{i-1} (\dot{u}_\theta)_{i-1} + (e_{yj})_i (\dot{u}_\theta)_i], \end{aligned} \quad (7b)$$

$$\begin{aligned} (f_\theta)_{i-1} = & c_{dj}(t) \cos^2 \alpha [(e_{yj})_{i-1} (\dot{u}_x)_{i-1} \\ & - (e_{yj})_{i-1} (\dot{u}_x)_i + (e_{yj})_{i-1}^2 (\dot{u}_\theta)_{i-1} \\ & - (e_{yj})_i (e_{yj})_{i-1} (\dot{u}_\theta)_i], \end{aligned} \quad (7c)$$

$$\begin{aligned} (f_\theta)_i &= c_{dj}(t) \cos^2 \alpha [-(e_{yj})_i (\dot{u}_x)_{i-1} + (e_{yj})_i (\dot{u}_x)_i \\ &\quad - (e_{yj})_{i-1} (e_{yj})_i (\dot{u}_\theta)_{i-1} + (e_{yj})_i^2 (\dot{u}_\theta)_i]. \end{aligned} \quad (7d)$$

So, the equation of motion of the building with one added damper can be expressed as:

$$\mathbf{M}\ddot{\mathbf{U}} + \mathbf{C}\dot{\mathbf{U}} + \left\{ \begin{array}{c} 0 \\ \vdots \\ 0 \\ (-1)_{i-1} \\ (+1)_i \\ 0 \\ \vdots \\ 0 \\ -(e_y)_{i-1} \\ (e_y)_i \\ 0 \\ \vdots \\ 0 \end{array} \right\}_{3n \times 1} f_j + \mathbf{K}\mathbf{U} = -\mathbf{M}\mathbf{I}\ddot{\mathbf{U}}_g(t), \quad (8)$$

where  $f_j$  is the damping force of the  $j$ th damper installed in a diagonal brace with the angle of  $\alpha$  to the horizontal axis and defined in Equation 7b.

Equation 8 can also be written as:

$$\mathbf{M}\ddot{\mathbf{U}} + \mathbf{C}\dot{\mathbf{U}} + \mathbf{K}\mathbf{U} = \mathbf{d}f_j - \mathbf{M}\mathbf{l}\ddot{\mathbf{U}}_g(t), \quad (9)$$

where  $\mathbf{d}$  is implicitly given in Equation 8.

Equation 9 relates to the case when only one damper,  $j$ , is added to the building. The generalized form of this equation, when  $m$  and  $k$  dampers are used in  $x$  and  $y$  directions, respectively, is represented as:

$$\mathbf{M}\ddot{\mathbf{U}} + \mathbf{C}\dot{\mathbf{U}} + \mathbf{K}\mathbf{U} = \mathbf{D}\mathbf{F} - \mathbf{M}\mathbf{I}\ddot{\mathbf{U}}_g(t), \quad (10)$$

where matrix  $\mathbf{D}$  is obtained according to the numbers and placement of the dampers and represented as [27]:

$$\mathbf{D} = \left[ \begin{array}{ccccccccc} -1 & & 0 & & \cdots & & & & \\ & 0 & \vdots & & & & & & \\ & \vdots & & 1 & & \ddots & & & \\ & & -1 & & & & & & \\ & & 0 & & & & 1 & & \\ \vdots & & & & & & & & \\ \vdots & & \cdots & & & & -1 & & 0 \\ & & & & & & & -1 & \\ & & & & & & & 0 & \\ & & & & & & & \vdots & \\ & & & \vdots & & & & & \\ & & & \vdots & & & & & \\ - (e_{y1})_1 & 0 & \cdots & 0 & & 0 & - (e_{x1})_1 & & \\ 0 & \vdots & & \vdots & & \vdots & 0 & & \\ \vdots & & (e_{yj})_{i-1} & 0 & & & \vdots & & \\ \vdots & & - (e_{yj})_i & \ddots & & & & & \\ & & 0 & & & & & & \\ & & \vdots & & (e_{ym})_{11} & & & & \\ 0 & 0 & & - (e_{ym})_{12} & 0 & & & & \\ & & & & & & & & \\ & \cdots & & 0 & & & & & \\ & & & \vdots & & & & & \\ & & & \vdots & & & & & \\ & & & & & 0 & & & \\ & 0 & \cdots & & & & & & \\ 0 & & \cdots & & & & & & \\ & 1 & & \ddots & & & & & \\ -1 & & & & & & & & \\ 0 & & & & & 1 & & & \\ \cdots & & & & & -1 & & & \\ 0 & \cdots & & 0 & & & & & \\ \vdots & & & & & & & & \\ (e_{xj})_{i-1} & & & & & & & & \\ - (e_{xj})_i & & \ddots & & & & & & \\ 0 & & & & & & & & \\ \vdots & & & & & & & & \\ \vdots & & & & (e_{xk})_{11} & & & & \\ 0 & & & - (e_{xk})_{12} & & & & & \end{array} \right]_{3N \times (m+k)} \quad , \quad (11)$$

and vector  $\mathbf{F}$  includes all the forces produced by

dampers, given as:

$$\mathbf{F} = \begin{Bmatrix} f_{x,1} \\ f_{x,2} \\ \vdots \\ f_{x,m-1} \\ f_{x,m} \\ f_{y,1} \\ f_{y,2} \\ \vdots \\ f_{y,k-1} \\ f_{y,k} \end{Bmatrix}_{(m+k) \times 1} \quad (12)$$

In order to solve Equation 10, it is written in state-space form as:

$$\dot{\mathbf{Z}} = \mathbf{A}\mathbf{Z} + \mathbf{H}\mathbf{F} + \mathbf{B}\mathbf{W}, \quad (13)$$

where  $\mathbf{A}$  is the state matrix;  $\mathbf{F}$  is the time-varying damping control force vector;  $\mathbf{Z}$  is the state vector; and  $\mathbf{W}$  is the disturbance vector. Variables in this equation are defined in the following:

$$\begin{aligned} \mathbf{A} &= \begin{bmatrix} \mathbf{0} & \mathbf{I} \\ -\mathbf{M}^{-1}\mathbf{K} & -\mathbf{M}^{-1}\mathbf{C} \end{bmatrix}, & \mathbf{B} &= \begin{bmatrix} \mathbf{0} \\ \mathbf{I} \end{bmatrix}, \\ \mathbf{W} &= -\mathbf{I}\ddot{\mathbf{U}}_g(t), & \mathbf{Z} &= \begin{Bmatrix} \mathbf{U} \\ \dot{\mathbf{U}} \end{Bmatrix}, \\ \mathbf{H} &= \begin{bmatrix} \mathbf{0} \\ \mathbf{M}^{-1}\mathbf{D} \end{bmatrix}, \end{aligned} \quad (14)$$

where  $\mathbf{0}$  is a zero matrix, and  $\mathbf{I}$  is an identity matrix.

In the semi-active control of the buildings, damping forces are produced based on feedback from sensors that measure the excitations/response of the structure, and with a damping command from the computer [15].

In this study, the Linear Quadratic Regulator (LQR) control algorithm is used to design the damping command. In this algorithm, the control force is found, such that the performance index,  $J$ , is minimized [14]:

$$J = \int_0^\infty (\mathbf{Z}^T \mathbf{Q} \mathbf{Z} + \mathbf{F}^T \mathbf{R} \mathbf{F}) dt, \quad (15)$$

where:

$$\begin{aligned} \mathbf{Q} &= \begin{bmatrix} \mathbf{Q}_v & \mathbf{0} \\ \mathbf{0} & \mathbf{0} \end{bmatrix}, & \mathbf{Q}_v &= \text{diag}(1), \\ \mathbf{R} &= 10^{-q} \text{diag}(1), \end{aligned} \quad (16)$$

where  $q$  is a weighting coefficient and should be calculated for the building. In the numerical analysis, it is shown that by increasing the value of  $q$ , the responses of the building decrease, while the damping

force increases. Since the maximum capacity of the dampers used in this study is limited to 1000 kN, the optimal value of  $q$  should be obtained.

The minimization of the performance index,  $J$ , results in a control force vector of [14]:

$$\begin{aligned} \mathbf{F} &= -\mathbf{R}^{-1} \mathbf{B}^T \mathbf{P} \mathbf{Z} = -\mathbf{G} \mathbf{Z}, \\ \mathbf{G} &= \mathbf{R}^{-1} \mathbf{B}^T \mathbf{P} = [\mathbf{G}_d \quad \mathbf{G}_v], \end{aligned} \quad (17)$$

in which matrix  $\mathbf{G}$  is a feed-back gain, full matrix, with respect to the displacement and velocity. But, since the gain with respect to the displacement is negligible, velocity feed-back control is adapted and, therefore  $\mathbf{G}_d = 0$  [14].

Also,  $\mathbf{P}$  is the solution of the algebraic Riccati equation shown as [14]:

$$\mathbf{P}\mathbf{A} + \mathbf{A}^T \mathbf{P} + \mathbf{Q} - \mathbf{P}\mathbf{B}\mathbf{R}^{-1} \mathbf{B}^T \mathbf{P} = 0. \quad (18)$$

Substituting Equation 17 into Equation 13, the state-space equation is written as:

$$\dot{\mathbf{Z}} = (\mathbf{A} - \mathbf{H}\mathbf{G})\mathbf{Z} + \mathbf{B}\mathbf{W}. \quad (19)$$

## GENETIC ALGORITHMS

Genetic Algorithms (GAs), first proposed by Holland [28], are very effective and powerful stochastic search engines, based on the mechanism of natural selection and natural genetics processes that drive biological evolution. They can be used for solving a variety of optimization problems that are not well suited for standard optimization algorithms including problems in which the objective function is discontinuous, non-differentiable, stochastic or highly nonlinear.

In civil engineering design, especially in designing complex structures, optimization has a special importance and value. Basically, the optimization process finds a set of quantities for design parameters that yield optimal values of objective functions. Most optimization methods used in the design of structural vibration control systems are traditional, gradient-based search techniques. However, for these techniques, there are difficulties, both in selecting a suitable continuously differentiable cost function as well as incorporating the nonlinearities involved in the problem. Compared to these gradient-based methods, Genetic Algorithms (GAs) are very simple and powerful optimal search techniques, because GAs do not need a continuous and differentiable function to solve the problem, and are able to take into account the nonlinearities (if any) of the problem [29].

The genetic algorithms start from an initial population of individuals and repeatedly modify them. Each individual in the population is called a chromosome, representing a possible solution to a given problem.

Each chromosome is assigned a fitness score, according to how good a solution to the problem it is [30]. At each generation, GAs select highly fit individuals at random from the current population to be parents and uses them to produce the children for the next generation. Over successive generations, the population evolves toward an optimal solution.

The GAs use three main operations to create the next generation from the current population: selective reproduction, crossover, and mutation. In every generation, a set of strings is selected into the mating pool, based on its relatives' fitness. The fitter strings are given a better chance of passing their genes into the next generation. This process of natural selection is operated by selective reproduction. The crossover operation combines two parents and changes their genes to form new strings for the next generation. The mutation operation also applies random changes to the selected genes in the new generation [31].

The crossover operation used here is a one-cut-point, which randomly selects the cut point and exchanges the right parts of the parents to generate new strings. The probability of crossover is set as  $P_c = 0.25$ ; thus, in average 25% of chromosomes undergo the crossover process.

Mutation alerts one or more genes with a probability equal to the mutation rate. In this study, the probability of mutation is set as  $P_m = 0.01$ ; thus, in average 1% of all bits of the population undergoes mutation.

## NUMERICAL STUDY

In this study, for investigating the performance of semi-active fluid viscous dampers on the control of civil engineering structures subjected to earthquake excitations, a realistic 12-story building located in the city of Rasht, in Iran, is considered as a numerical problem. A typical floor plan of this building is shown in Figure 2. This building is a steel structure with braced frame systems and its height is about 33.0 m.

For this building, the mass and stiffness matrices are calculated using the matrix analysis procedure. The damping matrix of the building is also constructed from a linear combination of the mass and stiffness

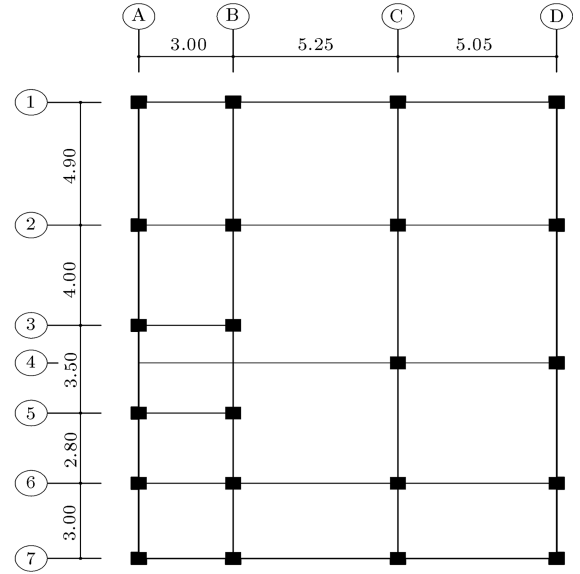


**Figure 2.** Typical floor plan of the building outline.

matrices (Rayleigh method). To calculate the proportionality coefficients, modal damping ratios of the first and middle modes are assumed to be about 5% of the critical values.

The building is analyzed for 15 earthquake acceleration records. Among these, 5 accelerograms are selected and scaled, according to the International Building Code (IBC) 2006 [32] for the design of seismic resistant buildings, and used for time history analysis of the building. More details of the 5 scaled accelerograms are given in Table 1.

First, by considering 22 semi-active fluid viscous dampers, the building is analyzed for the 5 scaled records. Figure 3 shows the placement of these dampers throughout the building. Dynamic characteristics of these dampers are given in Table 2 [14].

For determining the weighting coefficient,  $q$ , in the LQR control algorithm (Equation 16),  $q$  is varied from 4 to 10 and the maximum values of acceleration, displacement, story shear, and damping force are calculated for five selected values of  $q$  over the above range (Figure 4). The results show that by increasing values of  $q$ , the responses of the structure decrease but the damping force increases (Figure 4). So, because of limitation in the damping force (Table 2),  $q = 9$  is chosen in this analysis as the optimal value of  $q$ .

**Table 1.** Five acceleration records used for time history analysis.

Earthquake	Date	Station	Magnitude (Ms)	PGA (g)	Duration (sec)	Data Source
Northridge, California	1994/01/17	Montebello	6.7	0.128	21.82	USC
Chi-Chi, Taiwan	1999/09/20	CHY041	7.6	0.639	90.0	CWB
Imperial Valley, California	1979/10/15	El Centro	6.9	0.221	39.54	USGS
Kocaeli, Turkey	1999/08/17	Ambarli	7.8	0.249	150.39	CWB
Manjil, Iran	1990/06/20	Roudsar	7.7	0.093	21.88	NEIS

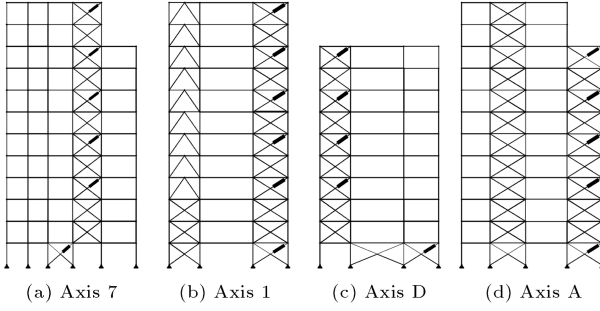


Figure 3. Configuration of dampers.

Table 2. Characteristics of the dampers [7].

Maximum Damping Force	1000 KN
Maximum Damping Coefficient	200 KN sec/mm
Minimum Damping Coefficient	1 KN sec/mm
Weight of Damper	1300 kg

By considering the above value for  $q$  and using MATLAB software, the equation of motion of the building with dampers is resolved and the maximum responses of the building are calculated for the five scaled earthquake acceleration records.

According to the standard IBC 2006 [32], in a time history analysis, if the number of earthquake acceleration records is less than 7, the maximum

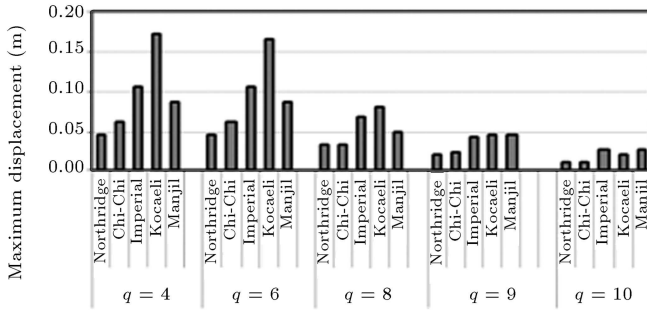
response of the building is to be chosen as the building response. Maximum responses of the building for five scaled earthquake accelerations are shown in Figure 5. As seen from the figure, displacements of the building are considerably reduced. In this case, the maximum reduction of top story displacement, acceleration and base shear force are about 63%, 38% and 40%, respectively. So, it is seen that semi-active fluid viscous dampers are very effective in reducing the building's seismic responses.

### Effect of Placement of Dampers on the Building's Responses

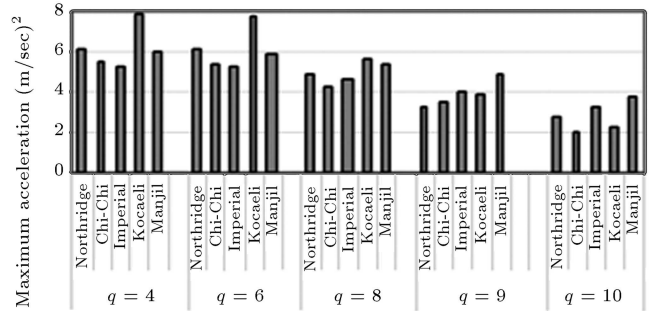
For investigating the effect of damper placement on building responses, 22 dampers are placed in 3 different locations in the building, as follows:

- All dampers are monotonically distributed in the height of the building (Figure 3);
- All dampers are placed in the upper floors of the building (Figure 6);
- All dampers are placed in the lower floors of the building (Figure 7).

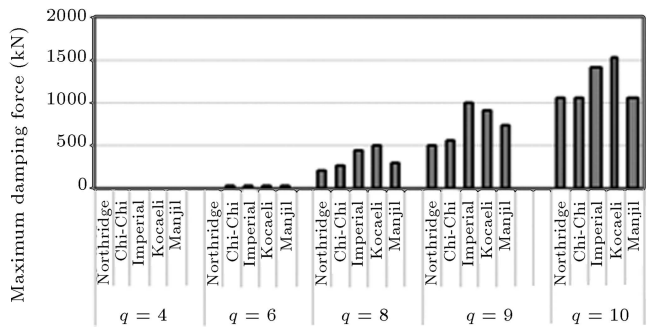
The building is analyzed for five scaled earthquake accelerations for the above three cases. In Figure 8, the maximum responses of the building for the Northridge



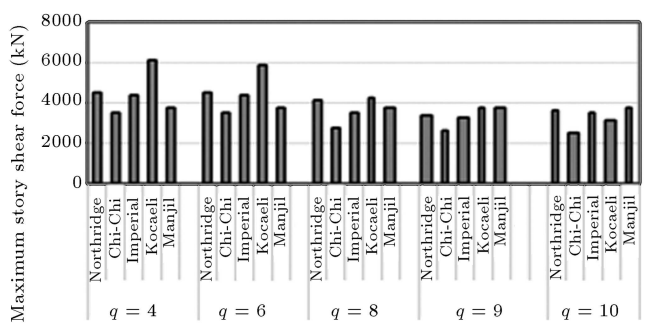
(a) Building maximum top story displacement



(b) Maximum top story acceleration



(c) Maximum damping force



(d) Maximum base story shear force

Figure 4. Maximum responses of the building for different values of  $q$ .

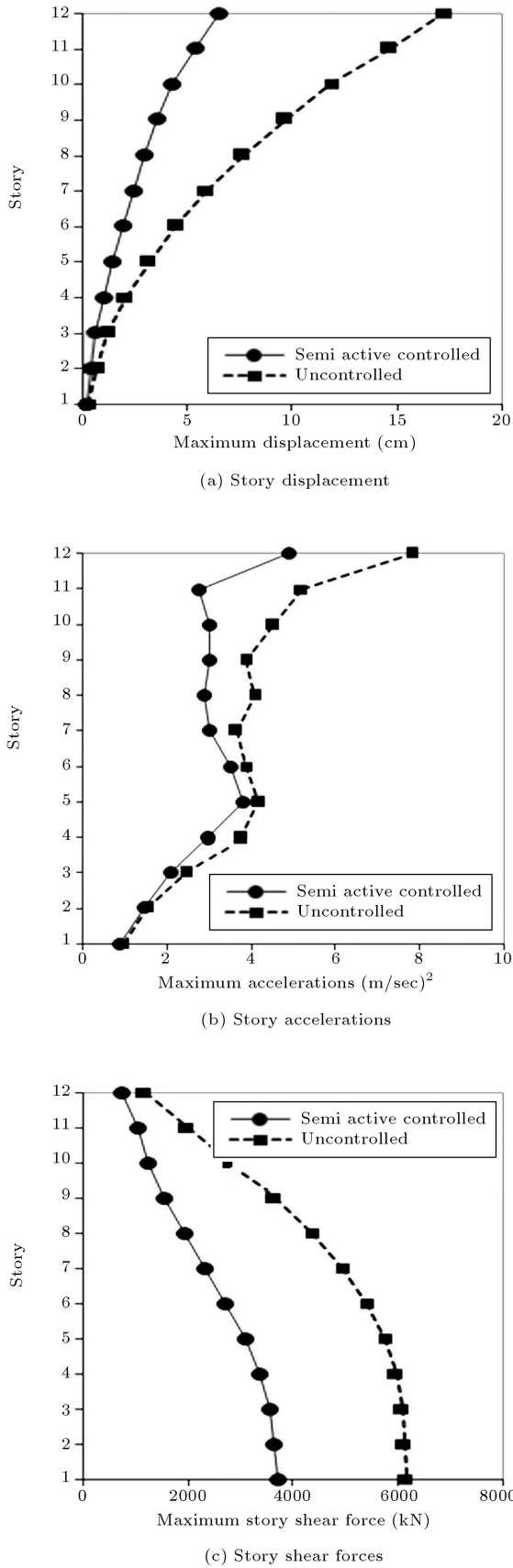


**Figure 5.** Maximum response of the building for five scaled earthquake accelerations.

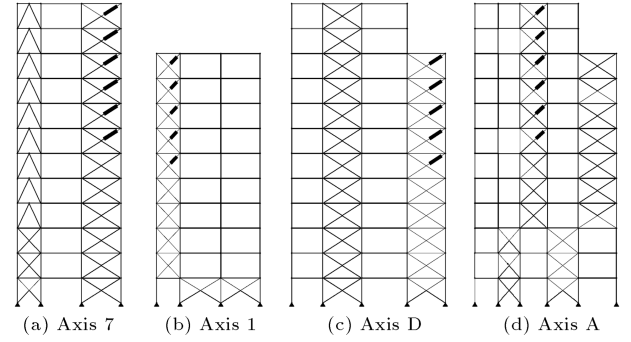


**Figure 6.** Configuration of dampers for case III.

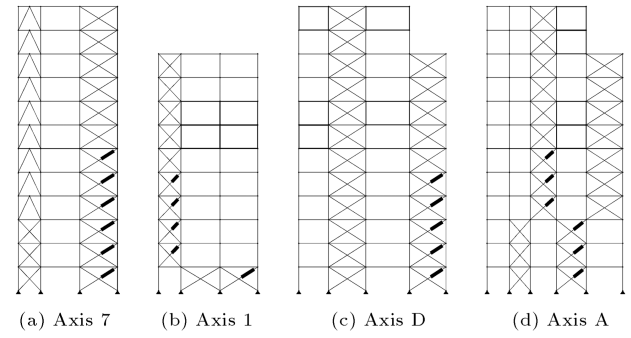


**Figure 7.** Configuration of dampers for case IV.

earthquake are shown. The results show that maximum displacement responses of the building are more sensitive to the location of the dampers, while the story shear forces are less sensitive to this parameter. Therefore, in order to study further the effect of this parameter on building responses, the location of the dampers is optimized in the next section, using genetic algorithms.

### Optimization of the Location and Number of Dampers Using Genetic Algorithms

In this section, using genetic algorithms, the required number and location of dampers are optimized to minimize the building's top story displacement, acceleration and base shear force.

In the example building, braces are located in axes 1, 2, 4, 5, 7, A, B, and D. Among these axes, those placed far from the center of mass are more proper for placing dampers, because, according to Equations 7a and 7b, damping force is directly related to  $e_x$  or  $e_y$ , and by increasing the values of  $e_x$  or  $e_y$  the amount of damping force increases. Thus, axes 1, 7, A and D are selected for placing the dampers and, therefore, 44 positions are available for this purpose. In order to model the location and number of dampers in the GA procedure, a variable  $X(i)$  is considered to show the presence of a damper in location  $i$  (Figure 9).  $X(i)$  is 1 when a damper is placed at location  $i$ , otherwise,  $X(i)$  is 0. The values of  $X(i)$  make a location matrix,  $\mathbf{L}$  [27].



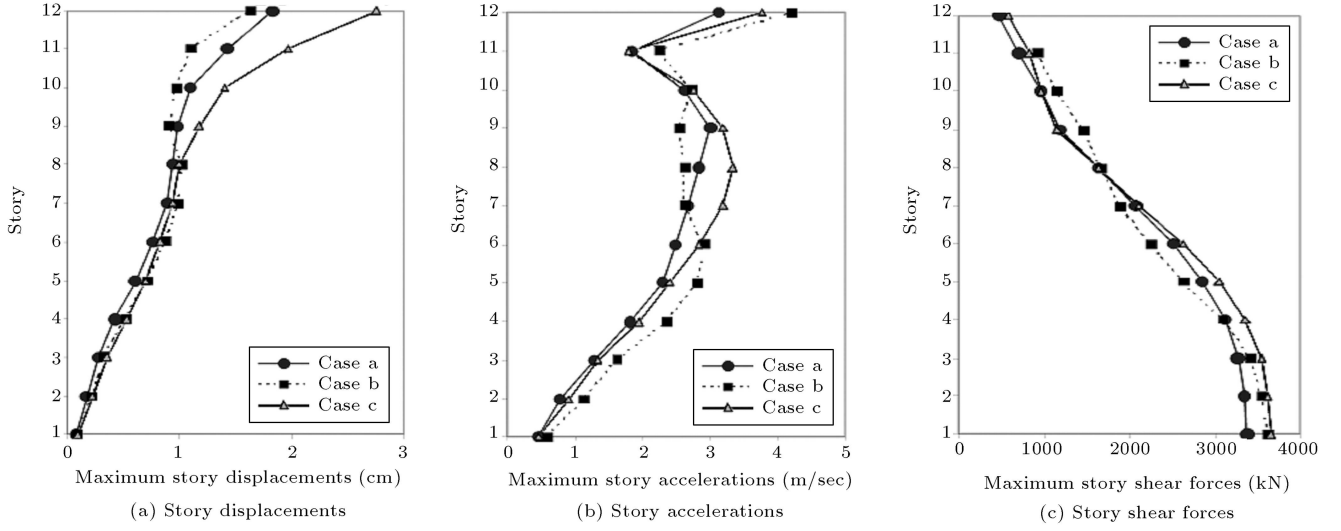


**Figure 8.** Maximum responses of the building in the Northridge earthquake for different location of dampers.

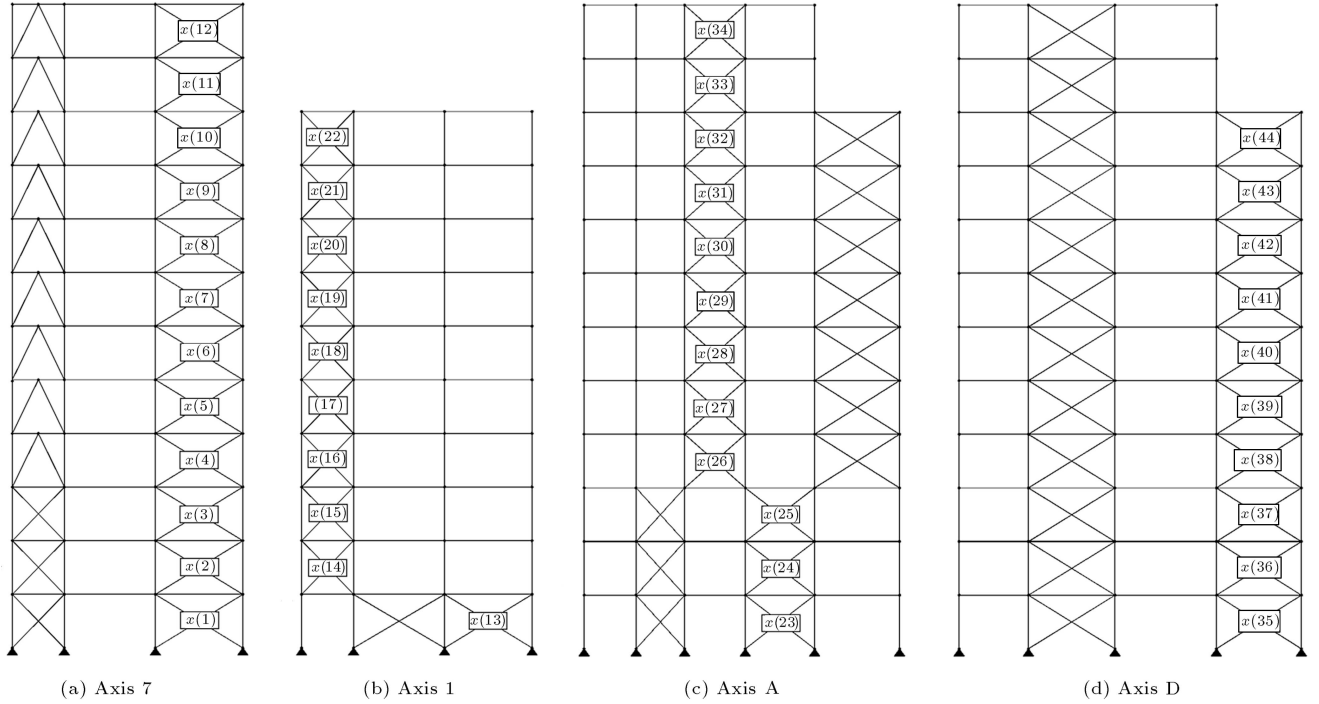


**Figure 9.** Assigned variables  $X(i)$  to the position of dampers.

The objective function is represented as:

$$g = \min \left[ \begin{array}{l} \frac{u_{\max, c}}{u_{\max, u}} \times 100 - 50 \\ \frac{\ddot{u}_{\max, c}}{\ddot{u}_{\max, u}} \times 100 - 65 \\ \frac{V_{\max, c}}{V_{\max, u}} \times 100 - 65 \end{array} \right]_{\max}, \quad (20)$$

in which  $u_{\max}$  and  $\ddot{u}_{\max}$  are the building's top story maximum displacement and acceleration, respectively;  $V_{\max}$  is the maximum base shear; and subscripts  $c$  and  $u$  denote the controlled and uncontrolled values. In defining the objective function, it is assumed that the upper limit of the reduction factors (ratio of controlled

to uncontrolled responses) for the maximum displacement, acceleration, and base shear of the building are to be about 50%, 65% and 65%, respectively.

According to above definition, and using the GA procedure, the optimized configuration of dampers is determined for 15 different earthquake acceleration records, mentioned in previous sections. It should be noted that for the GA optimizer, the following parameters are chosen:

Number of chromosomes = 50,

Number of generations = 300,

Probability of crossover,  $P_c = 0.25$

Probability of mutation,  $P_m = 0.01$ .

In Figure 10, the performance of the GA is shown for the Coalinga earthquake. According to the results obtained for the previously mentioned 15 earthquakes, the optimized location and number of dampers are obtained. The GA is performed for one earthquake acceleration record at each time, and the results of the location of the dampers, for all 15 acceleration records, are shown in Table 3. In this table, for a given earthquake acceleration, '1' indicates the presence of a damper at location  $X(i)$ , otherwise no damper is considered at that location. The final decision for damper placement is made based on the results of Table 3. For any location, if the number of 1 is more than 0, then one damper is considered at that location, otherwise no damper is chosen for that location.

Finally, based on the above procedure, 25 dampers are selected in optimal locations, and shown in Figure 11.

Moreover, in order to show the effectiveness of

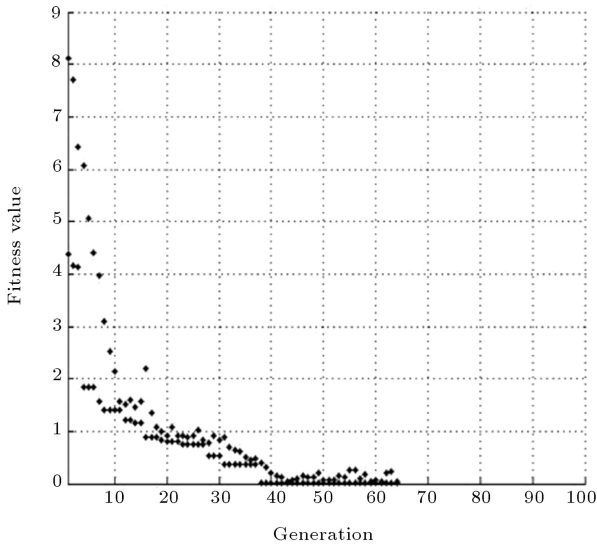


**Figure 10.** Performance of GA for Coalinga earthquake.

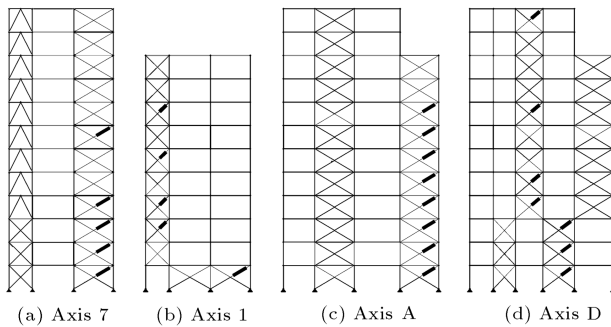


**Figure 11.** Optimized location of dampers using GA optimizer.

the optimized number and location of dampers, average values for the building's top story maximum displacement, acceleration and base shear force for the 15 earthquake accelerations are calculated for the following 4 cases and compared in Table 4:

- I. There are no dampers on the building (uncontrolled response);
- II. The building is controlled with 25 dampers all placed in their optimal positions (Figure 11);
- III. The building is controlled with 22 dampers all placed in the upper floors of the building (Figure 6);
- IV. The building is controlled with 22 dampers all placed in the lower floors of the building (Figure 7).

The results show that although, in point of top story displacement view, case III is more effective, it is not able to reduce the base shear force effectively. By comparing the results given in Table 4, it can be concluded that case II, in which the number and location of dampers are optimized using the GA, is in general more effective in reducing building responses.

## CONCLUSIONS

In this paper, the performance of semi-active fluid viscous dampers on the reduction of seismic responses of building structures is optimized using genetic algorithms. For this purpose, a realistic 12-story building located in the city of Rash, in Iran, is considered as a numerical problem. Equations of motion of a three-dimensional (3-D) model of the building, with added semi-active fluid viscous dampers, are written using an analytical procedure. Semi-active dampers are modeled by a linear spring-dashpot connected in parallel. For time history analysis of the building, 5 earthquake acceleration records are chosen, corrected for base-line errors, filtered for unwanted noise, and scaled based on the IBC 2006 standard. Then, using MATLAB software, the equations are resolved in state-space and the controlled and uncontrolled responses of the building are obtained.

Moreover, using genetic algorithms, the required number and location of dampers are optimized to minimize buildings' responses such as top story displacement, acceleration and base shear force. From the results of numerical study, it is found that:

1. Semi-active fluid viscous dampers are very effective in reducing the building's seismic responses. For the example building, a reduction of 74% is obtained on building a top story horizontal displacement.
2. In the LQR control algorithm, by increasing weighting coefficient  $q$ , the responses of the structure

**Table 3.** Results of GA performance for damper locations for 15 earthquake acceleration records.

Damper Locations	Earthquake Acceleration Records															Final Decision
	Northridge	Chi-Chi	Imperial Valley	Kocaeli	Manjil	Nahanni	Morgan Hill	Loma	Coalinga	San Fernando	Bam	Tabas	Gazli	Kobe	Zanjran	
$x(1)$	1	0	0	1	1	1	0	1	1	1	0	1	1	0	0	1
$x(2)$	1	1	1	0	1	1	1	1	0	0	1	1	0	1	0	1
$x(3)$	1	0	0	1	1	1	1	1	1	1	0	1	1	0	1	1
$x(4)$	1	1	1	1	0	1	1	1	1	1	1	0	1	0	0	1
$x(5)$	0	0	1	0	0	1	0	0	1	1	0	0	0	0	0	0
$x(6)$	0	0	0	1	0	1	0	0	0	0	1	0	0	1	0	0
$x(7)$	0	1	0	1	1	1	0	1	1	0	1	0	0	1	1	1
$x(8)$	0	0	1	0	1	0	0	0	0	0	0	0	0	0	1	0
$x(9)$	1	0	0	1	0	0	0	0	0	0	0	0	0	0	0	0
$x(10)$	0	0	1	0	0	0	0	0	1	1	0	0	0	0	0	0
$x(11)$	0	1	0	0	1	0	0	0	0	0	0	0	0	0	0	0
$x(12)$	0	0	1	1	0	0	0	1	0	0	0	1	1	0	1	0
$x(13)$	0	1	0	1	1	1	0	1	1	1	1	1	1	1	0	1
$x(14)$	0	1	1	0	0	1	0	1	1	1	0	0	0	0	0	0
$x(15)$	1	0	0	1	1	1	0	1	1	1	1	0	0	1	0	1
$x(16)$	1	0	1	1	0	1	1	1	1	1	1	0	0	1	0	1
$x(17)$	0	1	0	1	0	0	1	0	1	1	0	0	0	0	0	0
$x(18)$	1	0	0	1	1	1	0	1	1	0	1	1	0	0	1	1
$x(19)$	0	0	1	0	1	0	0	0	1	0	0	0	1	0	1	0
$x(20)$	0	1	1	1	0	1	0	0	0	0	1	0	1	1	1	1
$x(21)$	1	0	0	0	1	1	0	0	0	0	1	0	0	1	0	0
$x(22)$	0	0	0	0	0	0	1	0	0	0	0	1	1	0	0	0
$x(23)$	0	1	0	1	1	1	1	1	0	1	1	1	1	1	1	1
$x(24)$	1	0	1	1	0	1	1	1	1	1	0	1	1	0	1	1
$x(25)$	0	1	0	1	1	0	1	1	1	1	0	1	1	0	1	1
$x(26)$	1	1	1	1	0	1	1	1	0	1	1	1	1	0	1	1
$x(27)$	1	1	0	1	1	1	1	0	1	1	1	1	1	1	1	1
$x(28)$	0	0	0	0	1	1	1	0	0	0	0	0	0	1	1	0
$x(29)$	0	1	0	0	0	0	1	0	0	0	1	0	0	0	0	0
$x(30)$	1	1	1	1	0	1	1	0	1	1	0	1	0	1	0	1
$x(31)$	0	0	0	1	0	1	1	0	0	0	0	0	0	1	0	0
$x(32)$	0	0	0	1	1	1	1	0	0	0	0	1	1	1	0	0
$x(33)$	0	1	0	0	0	1	0	1	1	0	1	0	0	1	0	0
$x(34)$	1	1	1	1	0	1	0	1	1	1	1	1	1	1	0	1
$x(35)$	1	1	0	0	1	1	1	1	1	1	0	1	0	0	1	1
$x(36)$	1	1	1	0	0	1	0	1	1	1	1	1	1	1	1	1
$x(37)$	0	1	1	1	1	1	1	1	1	1	0	1	1	1	1	1
$x(38)$	1	1	1	0	1	1	1	1	1	0	1	1	1	1	1	1
$x(39)$	1	0	1	1	1	1	1	0	1	1	0	1	1	0	1	1
$x(40)$	1	1	0	1	1	1	1	1	0	1	1	0	0	0	1	1
$x(41)$	1	1	1	1	1	1	1	0	1	0	1	0	0	1	0	1
$x(42)$	1	0	1	1	1	1	1	1	1	0	1	0	0	1	0	1
$x(43)$	0	0	0	0	0	1	1	0	0	0	1	1	0	0	0	0
$x(44)$	0	0	0	0	1	0	0	0	0	0	0	0	1	0	0	0

**Table 4.** Responses of the building and their reduction ratio for four cases.

Responses of the Building	I	II	III	IV
Top story displacement (cm)	12.3	3.2	2.9	5.2
Top story displacement reduction ratio		74.0 %	76.4 %	57.7 %
Top story acceleration (m/sec <sup>2</sup> )	5.04	3.31	3.4	3.35
Top story acceleration reduction ratio		34.3 %	32.5 %	33.5 %
Base shear force (KN)	4047	2819	3405	3066
Base shear force reduction ratio		30.3 %	15.9 %	24.2 %

decrease, while the damping force increases. Due to the upper limitation of the damping force,  $q$  cannot be chosen as more than a specific value. For the example building,  $q$  is obtained to be about 9.

3. The location of dampers can have a significant effect on the response of the structures. Placing the dampers in the upper floors of the building effectively reduces the building's top story displacement, but they are not able to further reduce the base shear force by much. As well, placing the dampers in the lower floors of the building effectively reduces the base shear force, but does not have much effect on reduction of the building top story displacements. Therefore, the optimal number and location of the dampers can be evaluated using the GA to simultaneously reduce both the building's top story displacement and base shear force.

## REFERENCES

1. Joghataie, A. and Asbmarz, M.M. "Design method and feasibility study of fully actively controlled frames", *Scientia Iranica*, **11**(1&2), pp. 50-59 (2004).
2. Ggannadi-Asl, A. and Zahrai, S.M. "Seismic performance of TMDs in improving the response of MRF buildings", *Scientia Iranica*, **15**(1), pp. 21-33 (2008).
3. Kavand, A. and Zahrai, S.M. "Strong ground motion effects on seismic response reduction by TLCDs", *Scientia Iranica*, **15**(3), pp. 275-285 (2008).
4. Spencer, B.F. Jr and Sain, M.K. "Controlling buildings: A new frontier in feedback. IEEE control systems magazine", *Special Issue on Emerging Technologies*, Tariq Samad Guest Ed., **17**, pp. 19-35 (1997).
5. Khaje-Karamodin, A., Haji-Kazemi, H., Rowhani-manesh, A. and Akbarzadeh-Tootoonchi, M.R. "Semi-active control of structures using nero-inverse model of MR damping", *Scientia Iranica, Trasnsaction A*, **16**(3), pp. 256-263 (2009).
6. Aldemir, U. and Gavin, H.P. "Optimal semi-active control of structures with isolated base", *International Applied Mechanics*, **42**(2), pp. 235-240 (2006).
7. Gavin, H.P. and Aldemir, U. "Optimal control of earthquake using semi-active isolation", *Journal of Engineering Mechanics, ASCE*, **131**(8), pp. 769-776 (2005).
8. Alhan, C., Gavin, H.P. and Aldemir, U. "Optimal control: Basis for performance comparison of passive and semi-active isolation systems", *Journal of Engineering Mechanics, ASCE*, **132**(7), pp. 705-713 (2006).
9. Dyke, S.J. and Spencer, B.F. Jr "Seismic response control using multiple MR dampers", *Proceedings of the Second International Workshop on Structural Control*, Hong Kong, pp. 163-173 (1996).
10. Dyke, S.J. and Spencer, B.F. Jr "A Comparison of semi-active control strategies for the MR damper", *Proceedings of the International Conference on Intelligent Information Systems*, Bahamas, December, pp. 8-10 (1997).
11. Sack, R.L. and Patten, W. "Semi-active hydraulic structural control", *Proceedings of the Seventh International Workshop on Structural Control*, USC Publication No. CE-9311, pp. 417-431 (1994).
12. Sadek, F. and Mohraz, B. "Semi-active control algorithm for structures with variable dampers", *Journal of Engineering Mechanics, ASCE*, **124**, pp. 981-999 (1998).
13. Dyke, S.J., Spencer, B.F. Jr and Sain, M.K. "Carlson J.D. modeling and control of magnetorheological dampers for seismic response reduction", *Smart Materials and Structures*, **5**, pp. 565-575 (1996).
14. Kurata, N., Kobori, T., Takahashi, M., Niwa, N. and Midorikawa, H. "Actual seismic response controlled building with semi-active damper system", *Earthquake Engineering and Structural Dynamics*, **28**, pp. 1427-1447 (1999).
15. Symans, M.D. and Constantinou, M.C. "Semi-active control systems for seismic protection of structures: a state-of-the review", *Engineering Structures*, **21**, pp. 469-487 (1999).
16. Constantinou, M.C. and Symans, M.D. "Experimental and analytical investigation of seismic response of structures with supplemental fluid viscous dampers", in Technical Report NCEER-92-0032, National Center for Earthquake Engineering Research, Buffalo, New York (1992).
17. Soong, T.T. and Dargush, G.F., *Passive Energy Dissipation Systems in Structural Engineering*, John Wiley & Sons, England (1997).

18. Feng, Q. and Shinozuka, "Use of variable damper for hybrid control of bridge response under earthquake", in *Proceedings U.S. National Workshop on Struct. Control Responses*, USC Publication, No. CE-9013 (1990).
19. Kawashima, K., Unjoh, S. and Shimizu, K. "Experiments on dynamics characteristics of variable damper", in *Proc., Japan Nat. Symp. on Struct., Response Control* (1992).
20. Symans, M.D. and Constantinou, M.C. "Constitutive models for variable orifice fluid viscous dampers", in *Proceedings of the 12th Engineering Mechanics Conference*, La Jolla, California (1998).
21. Symans, M.D. and Constantinou, M.C. "Seismic testing of a building structure with semi-active fluid damper control system", *Earthquake Engineering and Structural Dynamics*, **26**, pp. 757-777 (1997).
22. Patten, W.N. "Field test of an intelligent stiffener for bridges at the I-35 Walnut Creek Bridge", *Earthquake Engineering and Structural Dynamics*, **28**, pp. 109-126 (1999).
23. Constantinou, M.C. and Symans, M.D. "Semi-active fluid viscous dampers for seismic response control", in *Proceedings of the First World Conference on Structural Control*, Pasadena, CA (1994).
24. Spencer, B.F. Jr "Technological frontiers of smart damping for protection of civil infrastructure", *US-Taiwan Workshop on Natural Disaster Reduction: Enabling Technologies and Integrated Mitigation Approaches*, Rockville, Maryland, USA (2002).
25. Chopra, A.K., *Dynamics of Structures: Theory and Applications to Earthquake Engineering*, 2nd Ed., Prentice-Hall (1998).
26. Lee, G.G., Liang, Z. and Tong, M., *Development of Semi-Active Structural Control System*, University at Buffalo, State University of New York (2001).
27. Mousanejad, T. "Optimization of semi-active viscous dampers control of seismically excited high rise buildings using genetic algorithms", MS Thesis, University of Guilan (2008).
28. Holland, J.H., *Adaptation in Natural and Artificial Systems*, Ann. Arbor, University of Michigan Press (1975).
29. Pourzeynali, S. and Zarif, M. "Multi-objective optimization of seismically isolated high-rise building structures using genetic algorithms", *Journal of Sound and Vibration*, **311**, pp. 1141-1160 (2008).
30. Gen, M. and Cheng, R., *Genetic Algorithms and Engineering Design*, John Wiley and Sons Inc. (1997).
31. Kim, Y.J. and Ghaboussi, J. "A new method of reduced order feedback control using genetic algorithms", *Earthquake Engineering and Structural Dynamics*, **28**, pp. 193-212 (1999).
32. International Building Code (IBC), published by International Code Council, Inc., U.S.A. (2006).